Editor's note: *The following four papers were originally presented at the First International Conference on Voice Physiology and Biomechanics, Evanston, IL, 28–31 May 1997. Anders Löfqvist*

A theoretical study of the hysteresis phenomenon at vocal fold oscillation onset–offset

Jorge C. Lucero[a)]
Departamento de Matemática, Universidade de Brasília, 70910-900 Brasília DF, Brazil

(Received 4 August 1997; accepted for publication 24 September 1998)

This paper presents a theoretical study on the differences in the biomechanical parameters of the vocal folds between oscillation onset and offset. The dynamics of the oscillation is analyzed from the perspective of the theory of nonlinear dynamical systems, using a mucosal wave model of the vocal folds with the subglottal pressure and the vocal fold half-width as control parameters. It is shown that the oscillation onset occurs through a Hopf bifurcation of the subcritical type, at which an unstable limit cycle is generated. Also, the oscillation offset occurs at a cyclic fold bifurcation, at which the unstable limit cycle and a stable limit cycle (the actual vocal fold oscillation) coalesce and cancel each other. Both bifurcations combine to form an ''oscillation hysteresis'' phenomenon, common in cases of flow-induced oscillations. An analytical expression for the onset/offset ratio of parameters is derived. The onset/offset ratio is in the range of 0.5–1, in agreement with the experimental evidence. This value depends on the phase delay in motion of the upper edge of the vocal folds versus the lower edge, and on the particular model adopted for airflow separation within the glottis. [S0001-4966(99)00201-5]

PACS numbers: 43.70.Aj, 43.70.Bk, 43.40.At, 43.40.Ga [AL]

INTRODUCTION

It is known that the biomechanical configuration of the vocal folds at oscillation onset is different from their configuration at oscillation offset. This difference has been observed for various parameters related to the vocal fold oscillation and under various experimental settings. For example, studies of excised larynges (Baer, 1981; Berry *et al.*, 1995) and physical models of the vocal fold mucosa (Titze *et al.*, 1995; Chan *et al.*, 1997) have shown that the subglottal pressure is lower at oscillation offset than at oscillation onset, when other biomechanical parameters (e.g., glottal width) are kept constant. Similar onset–offset differences have been also observed during the production of speech. Studies with subjects uttering vowel–voiceless consonant–vowel sequences have shown that the intraoral pressure is lower at the voice onset of the second vowel compared to the voice offset of the first vowel (Munhall *et al.*, 1994), the airflow is lower (Koenig and McGowan, 1996), the transglottal pressures is higher (Hirose and Niimi, 1987), and the glottal width is smaller (Hirose and Niimi, 1987).

According to this experimental evidence, the vocal fold configuration at oscillation onset seems to be always more restricted than the configuration at offset. When the geometry and other biomechanical parameters are fixed, as in the excised larynx experiments, then a larger subglottal pressure is required to start the oscillation. In the speech production experiments, if we assume that the subglottal pressure is approximately constant during the vowel–consonant–vowel sequence, then the experimental results indicate a larger vocal fold adduction at oscillation onset. Note that a smaller glottal width will increase the glottal aerodynamic resistance and therefore cause the observed larger transglottal pressure, smaller intraoral pressure, and lower airflow.

Why does this phenomenon occur? In this paper, we will look for its origin by examining the generation of the vocal fold oscillation from the perspective of the theory of nonlinear dynamical systems. In a previous work (Lucero, 1995), a describing function method (Siljak, 1969) was used to analyze the onset–offset difference in the subglottal pressure. The present work intends to offer an improved and more general description of this phenomenon, which might provide a theoretical basis for further studies. Considering that this paper is directed mainly to readers in the speech field, the mathematical techniques used in the paper which might be not familiar to some readers will be presented in detail.

I. VOCAL FOLD MODEL

Analysis will be based on a version of Titze's mucosal wave model (Titze, 1988) for the vocal fold oscillation. As shown in Fig. 1, we assume that during the oscillation the cover (epithelium and superficial layers of the vocal ligament) of the vocal folds propagates a surface mucosal wave in the direction of the airflow, and the body (deep layer of the vocal ligament and muscle) is stationary.

The cross-sectional areas at glottal entry a_1 and exit a_2 are approximated by

$$a_1 = 2L(x_0 + x + \tau\dot{x}), \tag{1}$$

$$a_2 = 2L(x_0 + x - \tau\dot{x}), \tag{2}$$

a)Electronic mail: lucero@mat.unb.br

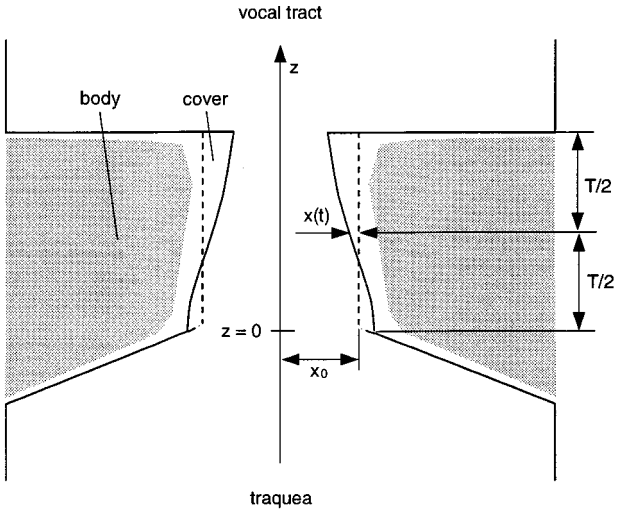

FIG. 1. Mucosal wave model (Titze, 1988).

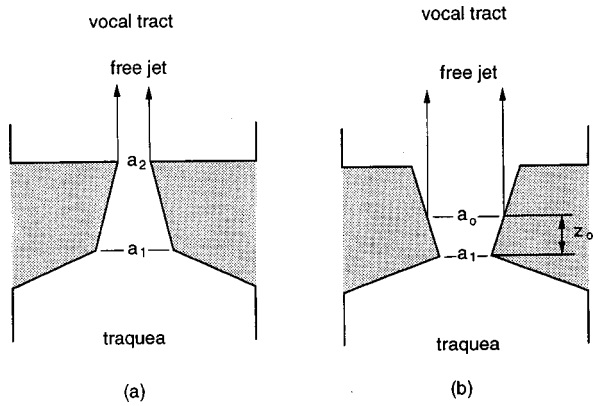

FIG. 2. Airflow separation from the glottis. (a) Convergent glottis, (b) divergent glottis.

where L is the length of the vocal fold in the antero–posterior direction, and τ is the time delay for the mucosal wave in traveling half the glottal width T (length of the glottal channel in the direction of the airflow). The motion of the vocal fold is described by the differential equation

$$m\ddot{x}+r\dot{x}+kx+P_g, \tag{3}$$

where x is the lateral displacement of the vocal fold at the midpoint of the glottis, m, r, and k, are the mass, damping, and stiffness of the oscillating portion of the vocal fold tissue per unit area of the medial surface of the vocal folds (LT), and P_g is the intraglottal pressure, equal to the mean of the glottal pressure $P(z)$ along the direction of the airflow (z axis in Fig. 1)

$$P_g=\frac{1}{T}\int_0^T P(z)dz. \tag{4}$$

Details on the derivation of the above equations may be found in Titze's paper (Titze, 1988).

For simplicity, we assume further that the supraglottal pressure is equal to the atmospheric pressure, the subglottal pressure P_s is constant, and the prephonatory glottal shape is rectangular (dashed line in Fig. 1).

The glottal aerodynamics is described following the boundary layer model by Pelorson and co-workers (Pelorson *et al.*, 1994, 1995) for high Reynolds numbers. This model appears to be valid for the range of typical values for the glottal flow (Re in the order of 3000), except when the glottis is narrow and near closure (in this case, a viscous model should be used).

The glottal flow is considered quasisteady and incompressible. The bulk of the flow is frictionless and laminar, except in the vicinity of the glottal walls (boundary layer) where viscous forces are large. Due to the abrupt area expansion at the glottal exit, the boundary layer separates from the glottal wall and causes a free jet stream downstream the glottis (Fig. 2). The point at which the flow detaches from the glottal wall is located at the exit of the glottis, in the case of a convergent glottis [Fig. 2(a)], or may move within the glottis, as it becomes divergent [Fig. 2(b)].

According to Pelorson *et al.*'s results (1994), in a divergent glottis the ratio between the glottal area a_0 at the point of airflow separation [see Fig. 2(b)] and the minimum glottal area (a_1) becomes asymptotically constant at high Reynolds numbers ($a_0/a_1\approx k_0$). In measurements on a physical model of the larynx with a cylindrical profile for the vocal folds, they obtained the approximate relation $a_0/a_1\approx 1.1$. For the present analysis, their equations (as they appear in Pelorson *et al.*, 1994) were solved assuming a linear variation of the glottal area along the glottis (z-axis in Fig. 1), and an approximate relation $a_0/a_1\approx 1.3$ was obtained. Hence, we assume as a first approximation that airflow separation occurs at the point where the glottal area is

$$a_0=\begin{cases} k_0a_1, & \text{if } a_2>k_0a_1, \\ a_2, & \text{if } a_2\leqslant k_0a_1, \end{cases} \tag{5}$$

where $k_0=1.3$. Coordinate z at the point of airflow separation has the value $z=z_0$, with

$$z_0=\frac{a_0-a_1}{a_2-a_1}\,T. \tag{6}$$

Downstream from the point of airflow separation, the air exits the glottis in a free jet and becomes turbulent. The turbulence dissipates all the kinetic energy of the flow and no pressure is recovered. Thus the pressure at the point of airflow separation is zero.

Upstream from the point of airflow separation, friction in the bulk of the flow may be neglected, and the flow described with the energy equation

$$P_s=\frac{\rho u^2}{2a_0^2}, \tag{7}$$

where P_s is the subglottal pressure, ρ is the air density, and u is the air flow volume velocity.

Finally, applying the energy equation between the point of coordinate z and the point of airflow separation z_0 to evaluate the pressure $P(z)$ (Titze, 1988) and integrating Eq. (4), we obtain

TABLE I. Parameter values of the mucosal wave model (Titze, 1988).

Parameter	Value
m	4.76 kg m^{-2}
r	1000 N s m^{-3}
k	2×10^6 N m^{-3}
L	1.4 cm
T	0.3 cm
$\omega=\sqrt{k/m}$	648.2 s^{-1}
δ	60°
$\tau=\delta/(2\omega)$	0.81 ms
ρ	1.15 kg m^{-3}

$$P_g = P_s \frac{z_0}{T}\left(1-\frac{a_0}{a_1}\right). \tag{8}$$

The dynamics of the model is then completely described by Eqs. (1), (2), (3), (5), (6), and (8). As standard values for the parameters, we adopt the values shown in Table I. In the table, $\delta=2\omega\tau$ is the phase delay in motion of the upper edge of the vocal folds in relation to the lower edge. These values will be used throughout the analysis, except where indicated otherwise.

We must be aware that this model contains gross simplifications of the vocal fold dynamics. Particularly, it neglects three factors consistent with the quasi-steady flow assumption: (1) viscous losses, which may become significant when the glottis is narrow and the glottal flow is low (note that the boundary layer model contains the assumption of a high Reynolds number); (2) glottal exit rounding effects on the pressure distribution in the glottis (Guo and Scherer, 1993); and (3) the actual point of action of the resultant glottal pressure (P_g), which should be lower than the glottal midpoint (Guo and Scherer, 1993). Preliminary analyses including viscous losses [following Pelorson *et al.*'s model (1994)] have shown no significant variation of the present results for the range of parameters considered here, e.g., a wide open glottis at the prephonatory position. This fact is consistent with a previous analysis on the optimal glottal configuration (Lucero, 1997), which shows that in a wide glottis airflow separation effects are much larger than viscous losses, and hence the later may be neglected as approximation. However, the situation may be different in a glottis near closure (as in the case of a pressed voice onset). The above simplifications are intended to reduce the model to the basic oscillatory dynamics, neglecting details not relevant to the present study.

II. EQUILIBRIUM POSITION AND STABILITY (PREVIOUS RESULTS)

The first step in the analysis is to determine the equilibrium positions of the vocal folds and their stability. Setting to zero the time derivatives, from Eqs. (1) and (2) we obtain $a_1=a_2$. Since the glottis is rectangular, there is no airflow separation within the glottis, hence $a_0=a_2$ and $z_0=T$. Solving the resultant equations for x, we find that there is only one equilibrium position and it is located at the initial position $x=0$.

The stability of the equilibrium position may be next analyzed taking only the linear part of the equation of motion in the neighborhood of the equilibrium position (Minorsky, 1962; Guckenheimer and Holmes, 1983). Since the oscillation has a small amplitude in that neighborhood and hence the glottis is near rectangular, there is no airflow separation within the glottis and the glottal pressure simplifies to

$$P_g = P_s\left(1-\frac{a_2}{a_1}\right)=\frac{2\tau P_s\dot{x}}{x_0+x+\tau\dot{x}}. \tag{9}$$

Expanding this equation in a Taylor series and keeping only the linear terms, we obtain

$$P_g = r_g\dot{x}, \tag{10}$$

where

$$r_g=\frac{2\tau P_s}{x_0}. \tag{11}$$

We can see that the glottal pressure is proportional to the vocal fold velocity, and hence it acts as an aerodynamic damping with the coefficient r_g. Replacing in Eq. (3), we obtain the linearized equation of motion

$$m\ddot{x}+(r-r_g)\dot{x}+kx=0. \tag{12}$$

The roots of the characteristic equation are

$$s=-\frac{r-r_g}{2m}\pm\sqrt{\left(\frac{r-r_g}{2m}\right)^2-\frac{k}{m}}. \tag{13}$$

The real part of the roots are zero at

$$r-r_g=0. \tag{14}$$

For $r_g>r$ the roots have positive real parts and the equilibrium position is unstable. Note that under this condition, the total damping [coefficient for the $\dot{x}$ term in Eq. (12)] becomes negative. This negative sign implies a net transfer of energy from the airflow to the vocal folds, and so oscillation may start, as it will be shown later in Sec. IV A.

The condition expressed by Eq. (14) is the threshold condition for oscillation onset, at which the equilibrium position of the vocal folds becomes unstable and the oscillation is generated. Replacing Eq. (11) and solving, we may compute for example the oscillation threshold subglottal pressure

$$P_{s\text{-onset}}=\frac{rx_0}{2\tau}, \tag{15}$$

which is the minimum subglottal pressure required to start the oscillation. Similarly, we can consider an oscillation threshold glottal half-width

$$x_{0\text{-onset}}=\frac{2\tau P_s}{r}, \tag{16}$$

which is the maximum glottal half-width to start the oscillation.

This same stability analysis has been done in previous works using a variety of models and techniques (e.g., Ishizaka, 1981; Ishizaka and Matsudaira, 1972; Lucero, 1993, 1995; Steinecke and Herzel, 1995; Titze, 1988). However, analysis only shows that at threshold the equilibrium position

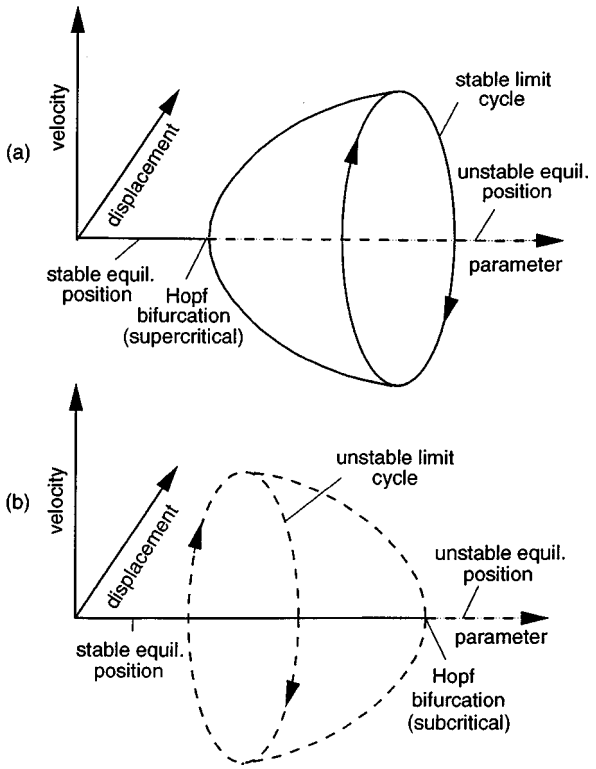

FIG. 3. The Hopf bifurcation. (a) Supercritical, (b) subcritical (Thompson and Stewart, 1986).

becomes unstable, and it says nothing about the generation of an oscillation. It is clear that an oscillation appears at threshold, as it can be shown by solving numerically the equations of motion. But exactly how is it generated? This issue is important in understanding the oscillation onset–offset dynamics, and will be considered in the following sections.

III. OSCILLATION ONSET: SUBCRITICAL HOPF BIFURCATION

A. The Hopf bifurcation

Let us briefly review how an oscillation may be generated from an equilibrium position. In the theory of nonlinear dynamical systems (Guckenheimer and Holmes, 1983; Minorsky, 1962; Thompson and Stewart, 1986), the qualitative change of dynamical behavior at a critical value of a parameter is called a bifurcation. At a Hopf bifurcation, an equilibrium position changes its stability and an oscillation (limit cycle) is generated.

Two types of Hopf bifurcations are possible. We illustrate them in Fig. 3, where we represent the dynamical behavior as a function of a control parameter (in the case of the vocal fold model, this parameter would be, e.g., the subglottal pressure or the glottal half-width). In the figures, a solid line represents stable equilibrium (a position or a limit cycle), and a dashed line represents unstable equilibrium. At the supercritical Hopf bifurcation [Fig. 3(a)], as the parameter increases a stable equilibrium position bifurcates into an unstable position and a stable limit cycle. This is the simplest case, and corresponds, e.g., to the well-known van der Pol oscillator. In the subcritical Hopf bifurcation [Fig. 3(b)], as the parameter increases a stable equilibrium position and an unstable limit cycle coalesce into an unstable equilibrium position. This case is more complex and appears in combination with other bifurcation phenomena. It is common in the flow-induced oscillation of structures, such as wind-induced oscillation of bridges (Thompson, 1982; Thompson and Stewart, 1986).

B. Hopf's theorem

To show the existence of a Hopf bifurcation at the oscillation onset threshold and determine its type, we may use Hopf's Theorem (Guckenheimer and Holmes, 1983). According to this theorem, first we have to verify that at the bifurcation, the system has a pair of pure imaginary roots and no other roots with zero real parts. This was done in the previous section. Next, we have to verify that, as the control parameter (e.g., the subglottal pressure) varies and passes the bifurcation value (i.e., the oscillation onset threshold), these roots cross the imaginary axes transversely. In mathematical terms,

$$\frac{d}{dP_s}\left[\mathrm{Re}\ s(P_s)\right]\Big|_{P_s=P_{s\text{-onset}}} \neq 0\,. \tag{17}$$

Introducing Eqs. (13) and (11), we obtain

$$\frac{d}{dP_s}\left[\mathrm{Re}\ s(P_s)\right]\Big|_{P_s=P_{s\text{-onset}}} = \frac{\tau}{mx_0} \neq 0. \tag{18}$$

Finally, we have to rewrite the equations of motion in the form

$$\begin{pmatrix} \dot{u} \\ \dot{v} \end{pmatrix} = \begin{pmatrix} 0 & -\omega \\ \omega & 0 \end{pmatrix} \begin{pmatrix} u \\ v \end{pmatrix} + \begin{pmatrix} f(u,v) \\ g(u,v) \end{pmatrix}, \tag{19}$$

where ω is a constant, $f(0,0)=g(0,0)=0$ (i.e., there is an equilibrium position at $u=0$, $v=0$), and $(\partial f/\partial u)(0,0)=(\partial f/\partial v)(0,0)=(\partial g/\partial u)(0,0)=(\partial g/\partial v)(0,0)=0$, and compute the parameter

$$K=\frac{1}{16}\left(f_{uuu}+f_{uvv}+g_{uuv}+g_{vvv}\right)+\frac{1}{16\omega}\left[f_{uv}\left(f_{uu}+f_{vv}\right)\right.$$
$$\left.-g_{uv}\left(g_{uu}+g_{vv}\right)-f_{uu}g_{uu}+f_{vv}g_{vv}\right], \tag{20}$$

where f_{uv} denotes $(\partial^2 f/\partial x\,\partial y)(0,0)$, etc. If $K\neq 0$ then the bifurcation is of the Hopf type, and a limit cycle is generated at the bifurcation. Further, if $K>0$ the bifurcation is subcritical, and if $K<0$ it is supercritical.

We can write the equations of motion in the form shown in Eq. (19) with the change of variables

$$u=-\omega x, \tag{21}$$

$$v=\dot{x}, \tag{22}$$

where $\omega=\sqrt{k/m}$, and letting

$$f(u,v)=0, \tag{23}$$

$$g(u,v)=-\frac{r}{m}\,v+\frac{2\tau P_s v}{m(-u/\omega+x_0+\tau v)}. \tag{24}$$

Note that $f(0,0)=g(0,0)=0$ as required by the theorem.

Next, we compute all the derivatives required by the theorem, and evaluate them at the equilibrium position $u=0$, $v=0$ and at the bifurcation condition $P_s=P_s-\text{onset}$. All of the derivatives of $f(u,v)$ are identically zero. The derivatives of $g(u,v)$ are

$$g_u=g_v=g_{uu}=0, \tag{25}$$

$$g_{uv}=\frac{r}{mx_0\omega}, \tag{26}$$

$$g_{vv}=-\frac{2\tau r}{mx_0}, \tag{27}$$

$$g_{uuv}=\frac{2r}{m\omega^2x_0^2}, \tag{28}$$

$$g_{vvv}=\frac{6\tau^2 r}{mx_0^2}, \tag{29}$$

and replacing in Eq. (20) we obtain finally

$$K=\frac{r}{8mx_0^2}\left(3\tau^2+\frac{1}{\omega^2}+\frac{\tau r}{m\omega^2}\right)>0. \tag{30}$$

The above result shows that oscillation onset is a subcritical Hopf's bifurcation, at which an unstable limit cycle is generated. This same conclusion will be reached repeating the same analysis with the glottal half-width x_0 as the control parameter

IV. HYSTERESIS AT OSCILLATION ONSET–OFFSET

A. Energy balance

In the previous section we found that the limit cycle generated at the oscillation onset bifurcation is unstable. An unstable limit cycle cannot be observed physically; if we could put the vocal folds exactly on the trajectory of this limit cycle, any infinitesimal perturbation would take them out of it. However, we know that the vocal folds are capable of a stable steady state oscillation. Moreover, if we solve the equations of motion numerically with a subglottal pressure just above the onset threshold value (as will be done later), we will find a stable limit cycle. We conclude then that the observed oscillation of the vocal folds (stable limit cycle) is not the same limit cycle generated at the Hopf bifurcation of the equilibrium position. Then, where does this stable limit cycle come from?

To answer this question, we have to study the system at large amplitude oscillations. Unfortunately, the vocal fold model is still complex and we cannot obtain a closed-form solution for the limit cycles. We will take then a more indirect approach, considering the exchange of energy between the glottal airflow and the vocal folds.

A criterion by Lièenard states that an oscillator reaches a steady state oscillation when the energies absorbed and dissipated in one cycle cancel out (Minorsky, 1983). In their oscillation, the vocal folds absorb energy from the airflow and dissipate energy in the tissues (Titze, 1988, 1994). Let us compute those energies.

The energy dissipated in the tissues is the work done by the damping force

$$W_r=\oint_{\text{cycle}} r\dot{x}\,dx=\int_0^{2\pi/\omega} r\dot{x}^2\,dt. \tag{31}$$

To compute this integral, we need an expression for $x(t)$. Let us assume as an approximation that the oscillation may be described by the sinusoid

$$x=A\sin\omega t. \tag{32}$$

Replacing into Eq. (31) and integrating, we obtain

$$W_r=\pi A^2\omega r. \tag{33}$$

The energy absorbed from the airflow is the work done by the glottal pressure

$$W_g=\oint_{\text{cycle}} P_g(x)dx=\int_0^{2\pi/\omega} P_g(t)\dot{x}\,dt. \tag{34}$$

Using again Eq. (32) for $x(t)$, we obtain

$$W_g=A\omega\int_0^{2\pi/\omega} P_g(t)\cos\omega t\,dt. \tag{35}$$

We can rewrite this equation in a similar form to Eq. (33)

$$W_g=\pi A^2\omega r_g, \tag{36}$$

where

$$r_g=\frac{1}{\pi A}\int_0^{2\pi/\omega} P_g(t)\cos\omega t\,dt \tag{37}$$

is an aerodynamic damping factor. This aerodynamic damping is equivalent to the one derived for the stability analysis of the equilibrium position [Eq. (11)], and we use the same symbol to denote it. Equation (37) is the general expression function of the oscillation amplitude, and it reduces to Eq. (11) when A tends to zero. [For small A, there is no airflow separation and P_g is given by Eq. (9). Introducing Eq. (32) and letting $A\to 0$, we obtain $P_g=(2P_s\omega\tau A\cos\omega t)/x_0$, and replacing in Eq. (37) and integrating we obtain Eq. (11).]

We will use r and r_g as normalized measures of the energies dissipated in the tissues and absorbed from the airflow, respectively, in one oscillation cycle. Lièenard's criterion will be then satisfied when $r=r_g$.

Figure 4 shows a numerical example of the normalized absorbed energy versus the oscillation amplitude, at various values of the airflow separation coefficient k_0. The solid line represents results using the above equations, and the dashed line represents results neglecting airflow separation in the glottis (i.e., setting $a_0=a_2$). The dashed line shows that the absorbed energy increases as the oscillation amplitude grows larger. This fact may be understood by considering that the transfer of energy from the airflow to the vocal folds is caused by the oscillation itself, so as the oscillation grows in amplitude, more energy can be transferred. However, for physical constraints the absorbed energy cannot grow to infinity. We see in the solid line that when airflow separation in the glottis is included, the slope of the curve changes at a certain oscillation amplitude. This amplitude is precisely the amplitude at which the point of airflow separation moves within the glottis. Airflow separation reduces the vocal fold surface through which the airflow transfers energy to the vocal folds, causing the decrease in the absorbed energy. If a

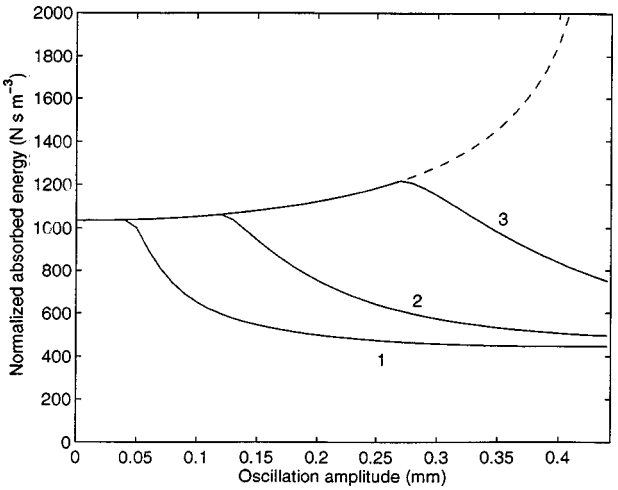

FIG. 4. Normalized absorbed energy versus oscillation amplitude, for $P_s = 320$ Pa, $x_0 = 0.5$ mm, and $k_0 = 1.1$ (1), 1.3 (2), 2 (3). At the right, the curves stop at the glottal closure.

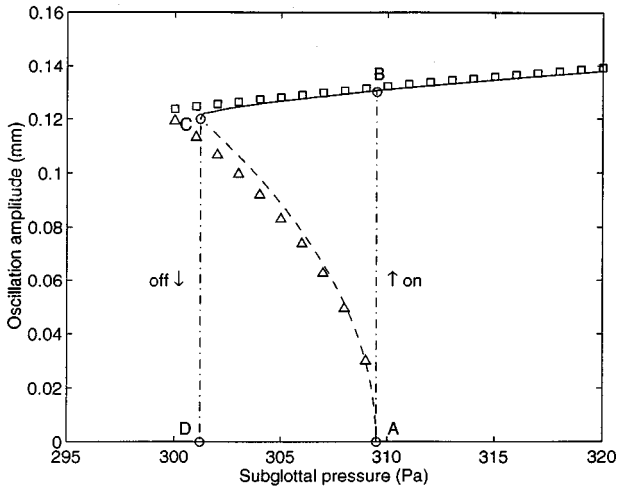

FIG. 6. Oscillation amplitude versus subglottal pressure for $x_0 = 0.5$ mm. Solid line: stable limit cycle, dashed line: unstable limit cycle. Point A: subcritical Hopf bifurcation, point C: cyclic fold bifurcation. A-B-C-D: oscillation hysteresis loop. Squares (stable limit cycle) and triangles (unstable limit cycle): results from direct solution of the equations of motion.

larger value of k_0 is adopted, then airflow separation within the glottis starts at a larger glottal divergence angle. In this case, the change of slope of the energy curve occurs at a larger oscillation amplitude, and the difference between the energy absorbed at zero amplitude and the maximum absorbed energy increases.

B. Oscillation hysteresis

Based on the previous results, we will examine the oscillation dynamics through numerical examples.

Figure 5 shows curves of normalized absorbed energy versus oscillation amplitude at various values of lung pressure. The normalized dissipated energy is $r = 1000$ N s m^{-3}, indicated in the plot with a dashed line.

Let us consider how the oscillation starts and stops. Assume that the vocal folds are initially at rest at the equilibrium position and hence the oscillation amplitude is zero. To start the oscillation, the absorbed energy has to be increased to a value above the dissipated energy. This will be accomplished increasing the lung pressure, for example, to 315 Pa (curve 4). Since the absorbed energy at zero amplitude is larger than the dissipated energy, the oscillation amplitude will grow following curve 4 until reaching a point of balance, at point A. This point represents a stable oscillation, or stable limit cycle. If a perturbation increases the oscillation amplitude, the absorbed energy becomes smaller than the dissipated energy, and the oscillation amplitude will return to the balance point. The opposite will happen if the perturbation decreases the oscillation amplitude. In this case, the absorbed energy becomes larger than the dissipated energy, and the oscillation amplitude will grow.

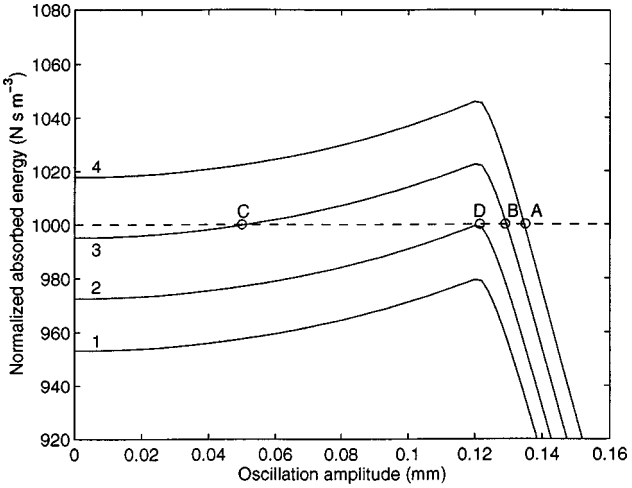

FIG. 5. Normalized absorbed energy versus oscillation amplitude, for $x_0 = 0.5$ mm and $P_s = 295$ Pa (1), 301 Pa (2), 308 Pa (3), 315 Pa (4). Dashed line: normalized dissipated energy. Points A and B: stable limit cycle, point C: unstable limit cycle, point D: cyclic fold bifurcation.

We can now decrease the subglottal pressure to a value lower than the value required to start the oscillation. For example, 308 Pa (curve 3). The oscillation amplitude will decrease to the new point of balance B. Note that there is also a second point of balance, point C. However, this is an unstable point. If a perturbation increases the oscillation amplitude, the absorbed energy becomes larger than the dissipated energy, and the oscillation will continue growing to point B. If the perturbation decreases the oscillation amplitude, the absorbed energy becomes smaller than the dissipated energy, and the oscillation will continue decreasing to the equilibrium point at zero amplitude. Point C represents then an unstable limit cycle, which is the limit cycle generated at the subcritical Hopf bifurcation.

At a subglottal pressure equal to 301 Pa (curve 2), both limit cycles coalesce at point D. Below this pressure (curve 1), there is no point of balance between the dissipated and absorbed energies, and hence no oscillation is possible. Point D is a bifurcation called cyclic fold, at which the unstable and stable limit cycles coalesce and canceled each other.

We can plot the points of energy balance taking the oscillation amplitude versus the lung pressure, as shown in Fig. 6. In this figure, the stable points (stable limit cycle) are plotted with solid line, and the unstable points (unstable limit cycle) with dashed line. The square and triangle symbols indicate results obtained by direct numerical solution of the

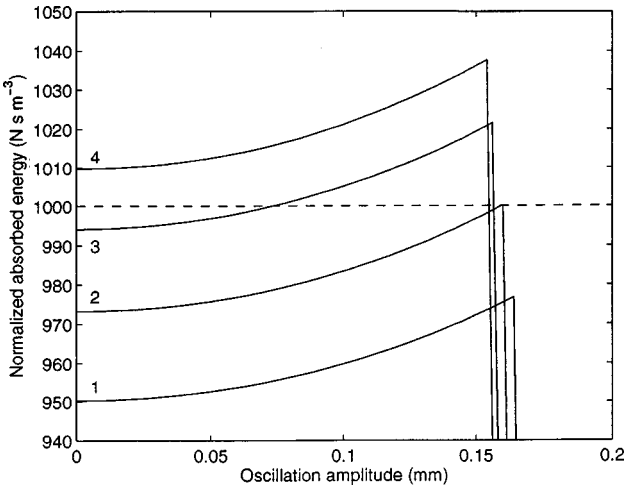

FIG. 7. Normalized absorbed energy versus oscillation amplitude, for $P_s = 400$ Pa and $x_0 = 0.68$ mm (1), 0.66 mm (2), 0.65 mm (3), 0.64 mm (4). Dashed line: normalized dissipated energy.

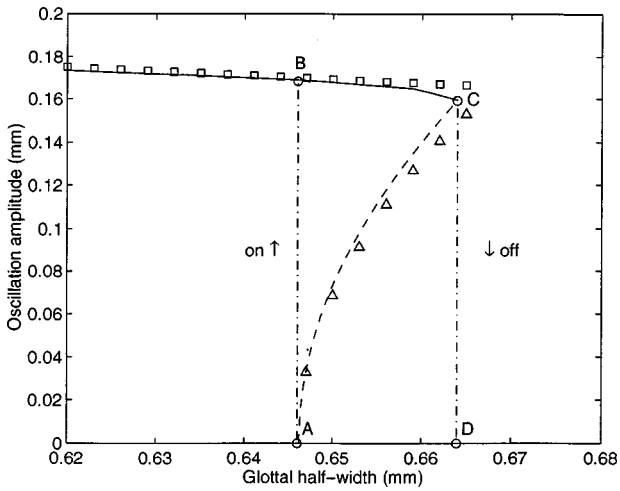

FIG. 8. Oscillation amplitude versus glottal half-width for $P_s = 400$ Pa. Solid line: stable limit cycle, dashed line: unstable limit cycle. Point A: subcritical Hopf bifurcation, point C: cyclic fold bifurcation. A-B-C-D: oscillation hysteresis loop. Squares (stable limit cycle) and triangles (unstable limit cycle): results from direct solution of the equations of motion.

equations of motion. The square is the amplitude of a stable limit cycle [the maximum value of $x(t)$] and the triangle is the amplitude of an unstable limit cycle. We can see no significant difference between the analysis and the numerical results, which validates the sinusoidal approximation for $x(t)$ [Eq. (32)] used in the energy analysis.

Increasing the subglottal pressure from zero, we need to reach point A to start the oscillation. Point A is the subcritical Hopf bifurcation found in Sec. III; at this point, the unstable limit cycle is generated and the equilibrium position becomes unstable. The subglottal pressure at this point is the oscillation onset threshold. As explained above, at this point the energy absorbed from the airflow becomes large enough to overcome the energy dissipated in the tissues. The oscillation will then start jumping to point B in the curve corresponding to the stable limit cycle. If we now reduce the lung pressure, the oscillation amplitude will decrease following the curve, until we reach point C. At this point, the stable and unstable limit cycles coalesce and disappear in a cyclic fold bifurcation. The oscillation will then vanish abruptly. The subglottal pressure at point D is then the oscillation offset threshold, and it is lower than the onset threshold. During this process, the oscillation amplitude follows a hysteresis loop A-B-C-D. The oscillatory behavior shown in the figure is the phenomenon called ''oscillation hysteresis'' by Appleton and Van der Pol (1922).

Note that according to Fig. 6, oscillation offset (i.e., the cyclic fold bifurcation) occurs at an oscillation amplitude at which there is a change in the slope of the curve absorbed energy versus oscillation amplitude, and recall that at this amplitude the point of airflow separation moves within the glottis (see explanation for Fig. 4). Hence, the analysis predicts that airflow separation within the glottis will occur in general during the oscillation cycle, except at the precise condition of offset threshold.

We can also consider the glottal half-width as control parameter. Figure 7 shows curves of normalized absorbed energy at various values of glottal widths. We can see a pattern for the curves similar to Fig. 5. In this case, to start the oscillation we have to decrease the glottal width, so that the absorbed energy at zero oscillation amplitude becomes larger than the dissipated energy. This will be accomplished at, for example, $x_0 = 0.64$ mm (curve 4). This curve has only one point of balance between the absorbed and dissipated energies, and it represents a stable limit cycle. The curve for $x_0 = 0.65$ mm (curve 3) has two points of balance, the left point represents an unstable limit cycle and the right point is a stable limit cycle. The curve for $x_0 = 0.66$ mm (curve 2) shows a cyclic fold bifurcation, at which both limit cycles coalesce. For larger glottal widths (curve 1) there is no point of energy balance and hence no oscillation is possible.

Figure 8 shows the points of energy balance taking the oscillation amplitude versus the glottal half-width. We can see also here a hysteresis loop A-B-C-D, similar to Fig. 6.

C. Onset–offset ratio

We will derive an analytical expression for the onset–offset ratio, to examine its relation to vocal fold parameters. Recall from Figs. 5 and 7 that the onset threshold corresponds to an oscillation amplitude $A = 0$, and the offset threshold corresponds to an oscillation amplitude at which the point of airflow separation moves within the glottis.

At this amplitude

$$a_2 = k_0 a_1 . \tag{38}$$

Using Eqs. (1), (2), and the sinusoidal approximation for $x(t)$ [Eq. (32)], and solving for the value of A such that there is a unique solution to Eq. (38), we obtain

$$a = \frac{k_0 - 1}{\sqrt{(k_0 - 1)^2 + \omega^2 \tau^2 (k_0 + 1)^2}}, \tag{39}$$

where $a = A/x_0$ is the normalized oscillation amplitude. Next, we compute the normalized absorbed energy at this oscillation amplitude. At this amplitude, there is no airflow separation within the glottis throughout the oscillation cycle, except at the point where the glottal divergence is maximum.

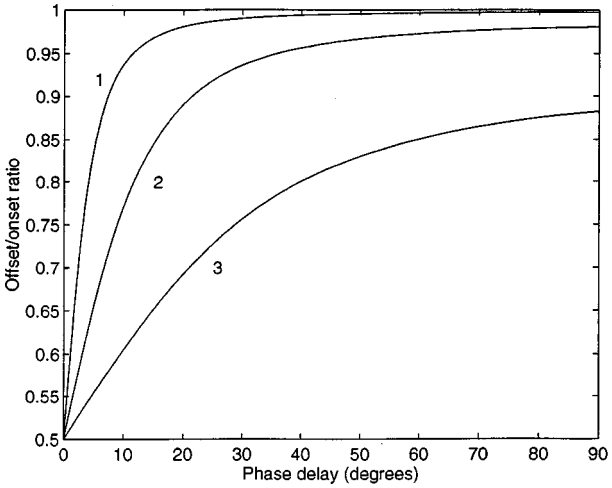

FIG. 9. Oscillation offset/onset ratio [Eq. (42)] versus phase delay, and $k_0 = 1.1$ (1), 1.3 (2), 2 (3).

Hence, we can use Eq. (9) for $P_g(t)$ (expression for no airflow separation in the glottis). Replacing in Eq. (37), and letting $\delta = 2\omega\tau$ be the phase delay of the upper edge of the vocal fold in relation to the lower edge, and $\theta = \omega t$, we obtain

$$r_g = \frac{2P_s\tau}{x_0}\,\Phi(\delta), \tag{40}$$

where

$$\Phi(\delta) = \frac{1}{\pi}\int_0^{2\pi} \frac{\cos^2\theta}{1 + a\,\sin\theta + 2\delta a\,\cos\theta}\,d\theta. \tag{41}$$

In the above equations, letting $r = r_g$, we obtain the point of balance between the absorbed and dissipated energies. Further, letting $a = 0$ we obtain the oscillation onset condition, and letting a equal to the value given by Eq. (39) we obtain the offset condition. Considering only the subglottal pressure and the glottal half-width as control parameters, we obtain the relation

$$\frac{(P_s/x_0)|_{\text{offset}}}{(P_s/x_0)|_{\text{onset}}} = \frac{1}{\Phi(\delta)}. \tag{42}$$

Figure 9 shows values of the offset/onset ratio versus the phase delay δ, and various values of the airflow separation coefficient k_0. Note that according to the above equations, the offset/onset ratio is only a function of these two parameters. In general, the offset/onset ratio varies between 0.5 and 1. This range is in agreement with experimental values (Baer, 1981; Berry *et al.*, 1995; Chan *et al.*, 1997; Hirose and Niimi, 1987; Koenig and McGowan, 1996; Munhall *et al.*, 1994; Titze *et al.*, 1995).

We see that at a given phase delay, the offset/onset ratio decreases (that is, the difference between onset and offset increases) as the airflow separation coefficient k_0 increases. Recall here the relation between coefficient k_0 and the glottal divergence angle at which airflow separation in the glottis starts, discussed for Fig. 4. Considering this result, we must note that previous models of the vocal fold oscillation (e.g., Herzel *et al.*, 1995; Steinecke and Herzel, 1995; Story and Titze, 1995) have assumed for simplicity that airflow separation in the glottis starts at zero degree of glottal divergence angle. This assumption is equivalent to a separation coefficient $k_0 = 1$, which leads to an offset/onset ratio equal to 1. Thus the present analysis predicts that those models should not be able to simulate the oscillation hysteresis phenomenon.

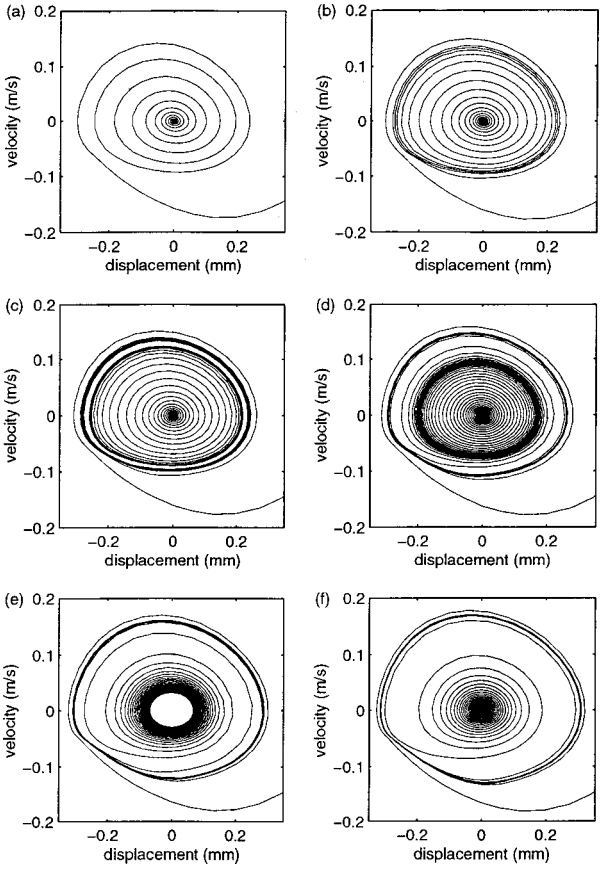

FIG. 10. Phase plane plots, for $x_0 = 0.5$ mm, $\delta = 30°$, $r = 2000$ N s m^{-3}, $k = 1\times10^6$ N m^{-3}, and $P_s = 750$ Pa (a), 786 Pa (b), 800 Pa (c), 830 Pa (d), 870 Pa (e), and 900 Pa (f). For clarity in the plots, no trajectory was plotted between the limits cycles in plot (c), and inside the internal limit cycle in plot (e).

D. Phase plane plots

The phase plane plots in Fig. 10 illustrate the dynamical behavior of the vocal folds, as the subglottal pressure is varied. They were obtained by direct solution of the equations of motion with numerical algorithms, and with parameter values selected to provide a clear plot. Plot (a) corresponds to a subglottal pressure below both thresholds, and shows a stable equilibrium position at the origin. In plot (b), we see that as the subglottal pressure increases and becomes near the offset threshold, the trajectory curves become closer together in a region around the equilibrium position, anticipating the cyclic fold bifurcation. Plot (c) corresponds to a subglottal pressure just above the offset threshold. We see that two limit cycles have appeared from a cyclic fold bifurcation. The internal limit cycle is unstable, and the external is stable. As the subglottal pressure continues to increase, we see in plots (d) and (e) that the internal unstable limit cycle becomes smaller and closes around the stable equilibrium

position at the origin. Finally, as the subglottal pressure passes the subcritical Hopf bifurcation at the onset threshold, unstable limit cycle and the stable equilibrium position coalesce and the equilibrium position becomes unstable. Plot (f) corresponds to a subglottal pressure above the onset threshold, we can see the unstable equilibrium position at the origin, surrounded by the stable limit cycle.

V. CONCLUSIONS

This analysis has shown that the differences observed at vocal fold oscillation onset versus offset may be described through the phenomenon of oscillation hysteresis (Appleton and van der Pol, 1922). This phenomenon is produced by a combination of two bifurcations: a subcritical Hopf bifurcation at oscillation onset and a cyclic fold bifurcation at oscillation offset, which occur at different values of the control parameters (e.g., glottal half-width or subglottal pressure). It is a consequence of the flow-induced nature of the vocal fold oscillation; in fact, it appears commonly in other cases of flow-induced oscillations (Thompson, 1982; Thompson and Stewart, 1986).

According to this analysis, the oscillation offset–onset ratio of vocal fold parameters is determined by the airflow separation from a divergent glottis. Airflow separation seems to be a central issue to understand the vocal fold oscillation dynamics. Pelorson *et al.* (1994, 1995) have already pointed out that airflow separation is the main mechanism for the airflow control by the movement of the vocal folds. Also, it seems to determine the optimal glottal angle for ease of phonation (Lucero, 1998). These results indicate the importance of an accurate modeling of the airflow separation, which should be a subject for further research efforts.

ACKNOWLEDGMENTS

These results were presented in partial form at the First International Conference in Voice Physiology and Biomechanics, in Evanston, IL, 29–31 May 1997. I am grateful to Kevin G. Munhall for his interest and support to this work, Ingo R. Titze for inspiring discussions on the vocal fold oscillation dynamics, Xavier Pelorson for his explanations on the airflow separation models, and Laura L. Koenig for discussions on her airflow measurements. This research was done while I was at the Speech Perception and Production Laboratory of the Department of Psychology, Queen's University at Kingston, and it was funded by NIH Grant No. DC-00594 from the National Institute of Deafness and other Communications Disorders and NSERC.

Appleton, E. V., and van der Pol, B. (**1922**). ''On a type of oscillation-hysteresis in a simple triode generator,'' Philos. Mag. **43**, 177–193.

Baer, T. (**1981**). ''Observation of vocal fold vibration: Measurement of excised larynges,'' in *Vocal Fold Physiology*, edited by K. N. Stevens and M. Hirano (University of Tokyo, Tokyo), pp. 119–133.

Berry, D., Herzel, H., Titze, I. R., and Story, B. (**1995**). ''Bifurcations in excised larynx experiments,'' NCVS Status and Progress Report **8**, 15–24.

Chan, R. W., Titze, I. R., and Titze, M. R. (**1997**). ''Glottal geometry and phonation threshold pressure in a vocal fold physical model,'' J. Acoust. Soc. Am. **101**, 3722–3727.

Guckenheimer, J., and Holmes, P. (**1983**). *Nonlinear Oscillations, Dynamical Systems, and Bifurcations of Vector Fields* (Springer-Verlag, New York), pp. 151–157.

Guo, C. G., and Scherer, R. C. (**1993**). ''Finite element simulation of glottal flow and pressure,'' J. Acoust. Soc. Am. **94**, 688–700.

Herzel, H., Berry, D., Titze, I., and Steinecke, I. (**1995**). ''Nonlinear dynamics of the voice: Signal analysis and biomechanical modeling,'' Chaos **5**, 30–34.

Hirose, H., and Niimi, S. (**1987**). ''The relationship between glottal opening and the transglottal pressure differences during consonant production,'' in *Laryngeal Function in Phonation and Respiration*, edited by T. Baer, C. Sasaki, and K. Harris (College-Hill, Boston), pp. 381–390.

Ishizaka, K. (**1981**). ''Equivalent lumped-mass models of vocal fold vibration,'' in *Vocal Fold Physiology*, edited by K. N. Stevens and M. Hirano (University of Tokyo, Tokyo), pp. 231–244.

Ishizaka, K., and Matsudaira, M. (**1972**). ''Theory of vocal cord vibration,'' Rep. Univ. Electro-Comm. Sci. Tech. Sect. **23**, 107–136.

Koenig, L. L., and McGowan, R. S. (**1996**). ''Voicing and aerodynamics of /h/ produced by men, women and children,'' J. Acoust. Soc. Am. **100**, 2689(A).

Lucero, J. C. (**1993**). ''Dynamics of the two-mass model of the vocal folds: Equilibria, bifurcations, and oscillation region,'' J. Acoust. Soc. Am. **94**, 3104–3111.

Lucero, J. C. (**1995**). ''The minimum lung pressure to sustain vocal fold oscillation,'' J. Acoust. Soc. Am. **98**, 779–784.

Lucero, J. C. (**1998**). ''Optimal glottal configuration for ease of phonation,'' J. Voice **12**(2), 151–158.

Minorsky, N. (**1962**). *Nonlinear Oscillations* (Krieger, Malabar), pp. 101–102 and 163–189.

Munhall, K. G., Löfqvist, A., and Scott Kelso, J. A. (**1994**). ''Lip-larynx coordination in speech: Effects of mechanical perturbations to the lower lip,'' J. Acoust. Soc. Am. **95**, 3605–3616.

Pelorson, X., Hirschberg, A., van Hassel, R. R., Wijnands, A. P. J., and Auregan, Y. (**1994**). ''Theoretical and experimental study of quasisteady-flow separation within the glottis during phonation. Application to a modified two-mass model,'' J. Acoust. Soc. Am. **96**, 3416–3431.

Pelorson, X., Hirschberg, A., Wijnands, A. P. J., and Bailliet, H. (**1995**). ''Description of the flow through *in-vitro* models of the glottis during phonation,'' Acta Acust. (China) **3**, 191–202.

Siljak, D. D. (**1969**). *Nonlinear Systems* (Wiley, New York), pp. 121–151.

Steinecke, I., and Herzel, H. (**1995**). ''Bifurcations in an asymmetric vocal fold model,'' J. Acoust. Soc. Am. **97**, 1874–1884.

Story, B. H., and Titze, I. R. (**1995**). ''Voice simulation with a body-cover model of the vocal folds,'' J. Acoust. Soc. Am. **97**, 1249–1260.

Thompson, J. M. T. (**1982**). *Instabilities and Catastrophes in Science and Engineering* (Wiley, New York), pp. 155–178.

Thompson, J. M. T., and Stewart, H. B. (**1986**). *Nonlinear Dynamics and Chaos* (Wiley, New York), pp. 108–131.

Titze, I. R. (**1988**). ''The physics of small-amplitude oscillation of the vocal folds,'' J. Acoust. Soc. Am. **83**, 1536–1552.

Titze, I. R. (**1994**). *Principles of Voice Production* (Prentice-Hall, Englewood Cliffs, NJ), pp. 81–105.

Titze, I. R., Schmidt, S. S., and Titze, M. R. (**1995**). ''Phonation threshold pressure in a physical model of the vocal fold mucosa,'' J. Acoust. Soc. Am. **97**, 3080–3084.